Crystallization Behavior of Polyhydroxybutyrate in Model Composites with Kenaf Fibers

A. Buzarovska,[1] G. Bogoeva-Gaceva,[1] A. Grozdanov,[1] M. Avella[2]

[1]*Faculty of Technology and Metallurgy, University of St. Cyril and Methodius, Rudjer Boskovic 16, 1000 Skopje, Macedonia*
[2]*Institute for Chemistry and Technology of Polymers, Via Campi Flegrei 34, 80078, Pozzuoli (Na) Italy*

Received 28 October 2005; accepted 21 January 2006
DOI 10.1002/app.24139
Publication online in Wiley InterScience (www.interscience.wiley.com).

ABSTRACT: The kinetics of the nonisothermal crystallization process of polyhydroxybutyrate in polyhydroxybutyrate/kenaf fiber model composites (with 80/20 and 70/30 w/w matrix/kenaf fibers) were investigated with differential scanning calorimetry. An analysis of the data was carried out with the Avrami, Ozawa, and modified Avrami and Ozawa models, as well as the Kissinger approach, for the determination of the crystallization activation energy. The Ozawa model was unsuitable for analyzing the nonisothermal data, whereas the other models described these systems very well. By the analysis of all the relevant parameters, the nucleation activity of the kenaf fibers was confirmed. The activation energies from the Kissinger method were evaluated to be 41.2, 32.6, and 26.3 kJ/mol for the pure polymer resin and 80/20 and 70/30 (w/w) polyhydroxybutyrate/kenaf fiber composites, respectively. © 2006 Wiley Periodicals, Inc. J Appl Polym Sci 102: 804–809, 2006

Key words: composites; crystallization; fibers

INTRODUCTION

The enormous production of plastic materials and the environmental problems related to increased plastic waste on huge scales have motivated many research groups to study biodegradable polymers.[1,2] Starch polymers, poly(lactic acid), poly(ε-caprolactone), poly(hydroxyalcanoate)s, and various types of polyesters are the most commonly investigated biopolymers that can be easily degraded or bioassimilated.[3,4]

Poly(3-hydroxybutyrate) (PHB) and its copolymers with valerate (PHBV) have received considerable scientific attention in the last 15 years.[5–7] These thermoplastics are materials with a high degree of crystallinity (x_c) and properties very similar to those of polyolefins. Their high price is the main limitation to their wider use, besides some of their unfavorable properties, such as brittleness.

For these reasons, PHB has been extensively studied in various polymer blends (mostly with synthetic polymers)[8–11] and as a polymer resin in natural composite materials.[12–15] In most of the published literature, attention has been paid to the miscibility, morphology, and crystallization behavior of PHB under isothermal conditions.[16,17]

In the case of fiber-reinforced PHB composites, many data are mainly related to the thermal and mechanical properties of the composites.[18] The nonisothermal crystallization behavior of this polymer resin in the presence of natural fibers has not been studied to a great extent.[19] The examination of the PHB crystallization behavior should enhance our understanding of the mechanical properties of its composites. The polymeric resin can nucleate on the surface of fibers and form a transcrystalline phase.[20] Mehl and Rebenfeld[21] showed that the incorporation of fibers into a PHB resin can affect both the crystallization kinetics and crystallinity of the resin. Biddlestone et al.[22] observed that the crystallization on rapid cooling in a mold develops at comparatively low temperatures and is subsequently followed by secondary crystallization at room temperature.

This article reports the influence of kenaf fibers on the nonisothermal crystallization behavior of a PHB resin in PHB/kenaf fiber composites. The experimental results were analyzed with the Avrami, Ozawa, Mo, and Jeziorny models.

THEORETICAL BACKGROUND

The well-known Avrami equation[23–25] is often used to describe the isothermal crystallization of polymers and can be applied to describe the nonisothermal crystallization process as well:[26,27]

Correspondence to: A. Buzarovska (abuzar@ian.tmf.ukim.edu.mk).

Contract grant sponsor: FP6-INCO-WBC; contract grant number: INCO-CT-2004-509185.
Contract grant sponsor: COST-Action P12 (financed by Ministry of Education and Science of Macedonia).

$$1 - X(t) = \exp(-kt^n) \quad (1)$$

where $X(t)$ is the relative crystallinity at time t, k is the crystallinity rate constant, and n is the Avrami exponent depending on the nucleation mechanism and the dimension of the crystal growth. For nonisothermal crystallization, the relative crystallinity is a function of temperature [$X(T)$], and time t is related to temperature T as follows:[28]

$$t = \frac{|T_o - T|}{\phi} \quad (2)$$

where T_o is the onset temperature at which crystallization begins ($t = 0$) and ϕ is the cooling rate. According to eq. (2), the horizontal axis observed in a differential scanning calorimetry (DSC) curve for nonisothermal crystallization data can be converted into a timescale. With eq. (1) in double logarithmic form and with a plot of $\log[-\ln(1 - X_t)]$ against $\log t$ for each cooling rate (where X_t is the relative crystallinity), the two adjustable parameters, k and n, can be calculated.

Considering the nonisothermal character of the process, Jeziorny[29] adequately corrected the kinetic parameter k, assuming constant ϕ, and thus obtained the parameter k_c, which characterizes the kinetics of nonisothermal crystallization:

$$\log k_c = \frac{\log k}{\phi} \quad (3)$$

The Ozawa method[30] is another approach commonly used for analyzing the nonisothermal crystallization of polymers. According to this theory, the nonisothermal crystallization process is a result of infinitesimally small isothermal crystallization steps, and the degree of conversion at temperature T can be calculated as follows:

$$-\ln(1 - X_t) = \frac{K^*(T)}{\phi^m} \quad (4)$$

where K^* is the cooling crystallization function (which is related to the overall crystallization rate) and m is the Ozawa exponent (which depends on the dimensions of crystal growth). Taking the double logarithm of eq. (4), we obtain the following form:

$$\log\{-\ln[1 - X(T)]\} = \log K^* - m\log\phi \quad (5)$$

Plots of $\log\{-\ln[1 - X(T)]\}$ versus $\log \phi$ are used to determine the K^* and m parameters from the intercept and slope, respectively. Mo et al.[31] proposed a model that is actually a modified method based on both the Avrami and Ozawa models. The well-known equation based on these two models is

$$\log\phi = \log F(T) - a\log t \quad (6)$$

where $F(T)$ refers to the value of the cooling rate, which is chosen at the unit of the crystallization time, when the measured system reaches a certain X_t value, and a is the ratio of n and m ($a = n/m$). The kinetic parameters $F(T)$ and a can be estimated from the intercept and slope of plots of $\log \phi$ versus $\log t$ at different cooling rates.

The activation energy (ΔE) of crystallization is often evaluated with the Kissinger method,[32] which defines ΔE as follows:

$$\frac{d[\ln(\phi/T_p^2)]}{d(1/T_p)} = \frac{\Delta E}{R} \quad (7)$$

where R is the universal gas constant and T_p is the peak crystallization temperature. ΔE can be determined from the slope of $\log(\phi/T_p^2)$ versus $1/T_p$.

EXPERIMENTAL

Materials

PHB with a molecular mass of 420,000 Da, a product of Biomer, was used as received. Kenaf fibers, kindly supplied by KEFI Italy (53–57% cellulose, 15–19% hemicellulose, 5.9–9.3% lignin, and 4.7% ash), were used without drying.

The model composites were prepared directly in DSC aluminum pans with two different ratios polymer matrix/kenaf fiber ratios (80/20 and 70/30 w/w), similarly to our previously published article.[33] The fibers in appropriate amounts were placed between two PHB films.

Methods

The nonisothermal crystallization behavior of PHB in the model composites was followed with a PerkinElmer DSC 7 differential scanning calorimeter (Wellesley, MA). The calibration of the instrument was performed with an indium standard.

The samples were heated from −20 to 190°C and kept at the final temperature for 5 min to erase the thermal history of the polymer resin. The samples were then crystallized at constant cooling rates of 40, 20, 15, 10, and 5°/min.

The morphology of the investigated composites was observed with a Leica polarized optical microscope (Wetzlar, Germany) equipped with a hot stage.

RESULTS AND DISCUSSION

The crystallization exotherms of the 80/20 (w/w) PHB/kenaf fiber composite at various cooling rates are presented in Figure 1. Similar DSC curves were

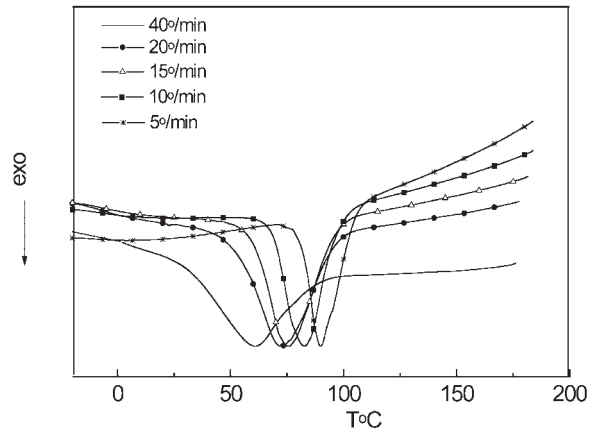

Figure 1 Crystallization exotherms during the nonisothermal crystallization of an 80/20 (w/w) PHB/kenaf fiber composite.

obtained for the pure PHB matrix and for the 70/30 (w/w) PHB/kenaf fiber composite. As expected, typical shifting of the crystallization peaks to lower temperatures could be observed with an increase in the cooling rates. This indicates that at slow cooling rates there is a sufficient time to activate nuclei at higher temperatures, whereas at faster cooling rates, the activation of nuclei occurs at lower temperatures. Some fundamental parameters taken from the cooling runs are listed in Table I: T_p and x_c [$x_c = \Delta H_f/\Delta H_f^o$, where ΔH_f is the enthalpy of fusion and ΔH_f^o (taken as 146 J/g[5]) is the enthalpy of melting of an ideal crystal]. Table I shows that at cooling rates between 20 and 5°/min, T_p increases with the content of kenaf fibers. The exception is the cooling rate of 40°/min, where T_p of the composites has a decreasing tendency, in comparison with the pure PHB matrix. In close relation to this are the estimated values for x_c given in the same table. Higher values of x_c are determined with an increasing amount of the natural fiber. This could be an indication of a nucleation effect of the kenaf fibers at lower cooling rates.

TABLE I
Fundamental Parameters Obtained from the Nonisothermal DSC Crystallization Curves of PHB and PHB/Kenaf Fiber Composites

	PHB		PHB/kenaf 80/20 w/w		PHB/kenaf 70/30 w/w	
ϕ (°/min)	T_p (°C)	x_c	T_p (°C)	x_c	T_p (°C)	x_c
40	64.5	18.7	60.4	23.6	59.4	21.7
20	70.2	42.2	72.2	42.6	72.8	41.6
15	75.4	44.0	76.6	45.3	80.2	46.5
10	81.3	49.3	82.8	50.3	88.5	53.2
5	88.1	52.0	89.9	55.3	96.2	58.2

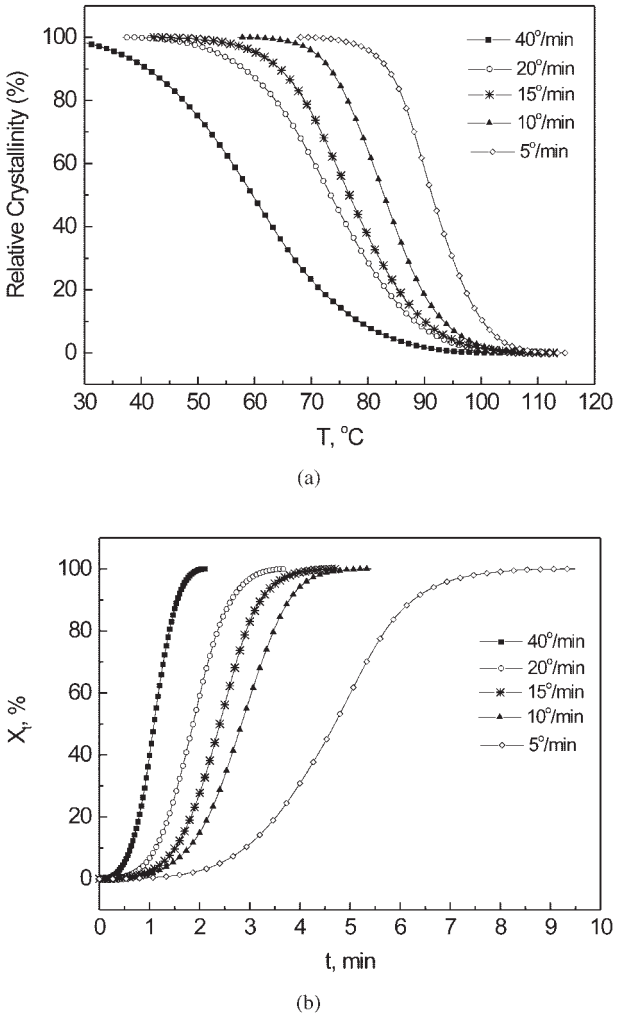

Figure 2 X_t as a function of (a) temperature and (b) time for an 80/20 (w/w) PHB/kenaf fiber composite.

Plots of X_t versus the temperature and time [converted with the conversion equation, eq. (2)] are illustrated in Figure 2. The linearity of these dependences is maintained from the initial stages of crystallization until very high X_t values (95–98%). This can be also confirmed by the plots of $\log[-\ln(1 - X_t)]$ versus $\log t$ for each cooling rate in Figure 3. Straight lines were obtained in the whole region of X_t. This could be an indication that the secondary crystallization process, during the dynamic nonisothermal crystallization, did not occur in these materials. The two adjustable Avrami parameters, derived from the slopes and intercepts of each line, were calculated and are collected in Table II. The corrected k_c constants, according to eq. (3), increase with the cooling rate but are almost unchanged for the PHB resin and for the two composites at a given cooling rate. This could be an indication that the crystallization rate is almost equal in all investigated systems. The Avrami parameter n ranges from 2 to 2.4 for PHB and for the two composites. The obtained values are almost identical to the n value cal-

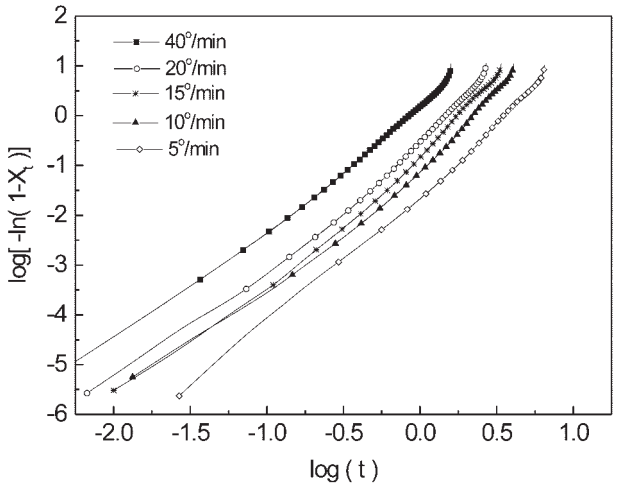

Figure 3 Avrami plots for an 80/20 (w/w) PHB/kenaf fiber composite.

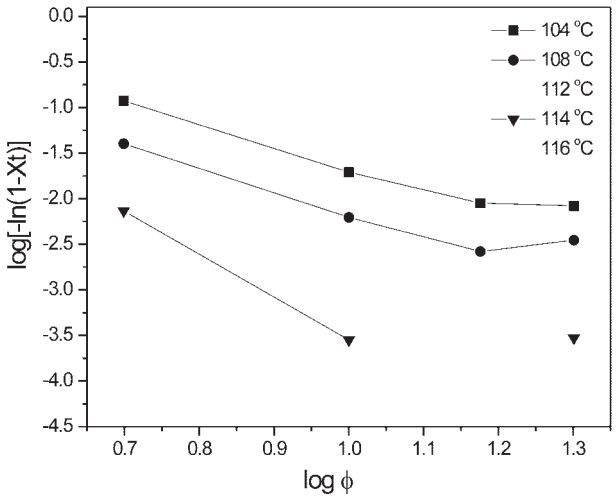

Figure 4 Ozawa plots at the indicated temperatures for a 70/30 (w/w) PHB/kenaf fiber composite: $\log[-\ln(1 - X_t)]$ versus $\log \phi$.

culated for the isothermal crystallization of PHB.[34] Dong et al.[35] reported higher values of n (between 3 and 4.9) for PHB, using the Avrami approach for nonisothermal crystallization.

A characteristic Ozawa plot is presented in Figure 4. The dependences of $\log\{-\ln[1 - X(T)]\}$ versus $\log \phi$ are very far from linearity, showing that this model is not useful for treating the experimental results. Similar graphs were obtained for the other investigated samples. Because the Ozawa approach can be defined as an ideal model for systems in which the crystallization process is mainly limited to region I (ignoring the secondary crystallization process), the deviation of the obtained results could be an indication that crystallization probably occurs beyond region I. If this is true, the already used Avrami equation adopted for the nonisothermal crystallization process will no longer be valid. Because the Avrami analysis shows a good fit with the experimental results, the reason for failing the Ozawa theory could be explained in terms of the quasi-isothermal nature of the treatment, which was also explained by Dong et al.[35]

Made with the modified Avrami and Ozawa approach proposed by Mo,[29] the characteristic plots of $\ln \phi$ versus $\ln t$ are presented in Figure 5. Linear correlations can be observed in all the investigated systems. The calculated $F(T)$ parameters (Table III) show that the $F(T)$ function increases with an increase in X_t. At low X_t values (up to 20%), the $F(T)$ function decreases with the kenaf fiber content, whereas for higher X_t values, the $F(T)$ parameter has a variable trend for PHB and the two investigated composites. This is more evidence that kenaf fibers act as nucleating sites for the crystallization of PHB and enhance its crystallization rate at low X_t values (up to 20%). For higher X_t values, the crystallization rates in all the investigated samples are logically lower than those obtained for low X_t values (Table III). As expected, the crystallization is retarded at higher X_t values. The a parameter has an almost constant value for all X_t values and ranges between 1.04 and 1.09 for PHB, 1.4 and 1.49 for the 80/20 (w/w) PHB/kenaf fiber composite, and 1.20 and 1.30 for the 70/30 (w/w) PHB/kenaf fiber composite. The derived Ozawa parameters from the relation $a = n/m$ are as follows: $m_{(\mathrm{PHB})} = 1.8$–2.0, $m_{(80/20\ \mathrm{PHB/kenaf})} = 1.50$–$1.60$, and $m_{(70/30\ \mathrm{PHB/kenaf})} = 1.60$–$1.90$.

TABLE II
Parameters Obtained from Avrami Analysis and Jeziorny Corrected Constants for PHB and Its Composites

	PHB				PHB/kenaf 80/20 w/w				PHB/kenaf 70/30 w/w			
ϕ (°/min)	log k	n	k_c	$t_{1/2}$	log k	n	k_c	$t_{1/2}$	log k	n	k_c	$t_{1/2}$
40	−0.91	2.0	0.95	0.8	−0.66	2.2	0.96	0.86	−0.19	2.4	0.98	0.86
20	−1.73	2.0	0.82	0.9	−1.33	2.2	0.86	0.91	−1.60	2.1	0.83	0.91
15	−1.79	2.1	0.76	0.9	−1.67	2.2	0.77	0.95	−1.53	2.3	0.79	0.94
10	−2.62	2.2	0.55	1.1	−1.78	2.3	0.66	1.02	−1.90	2.3	0.64	1.03
5	−2.33	2.2	0.34	1.4	−2.38	2.3	0.33	1.37	−2.56	2.0	0.31	1.49

$t_{1/2}$, the half time of crystallization defined as the time at which the degree of crystallinity is 50%.

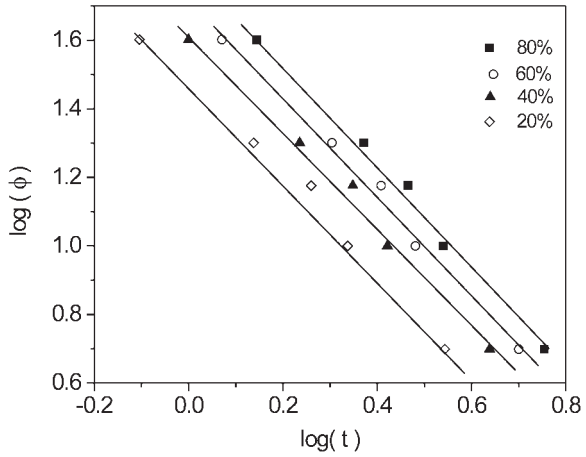

Figure 5 Plots of log ϕ versus log t for an 80/20 (w/w) PHB/kenaf fiber composite.

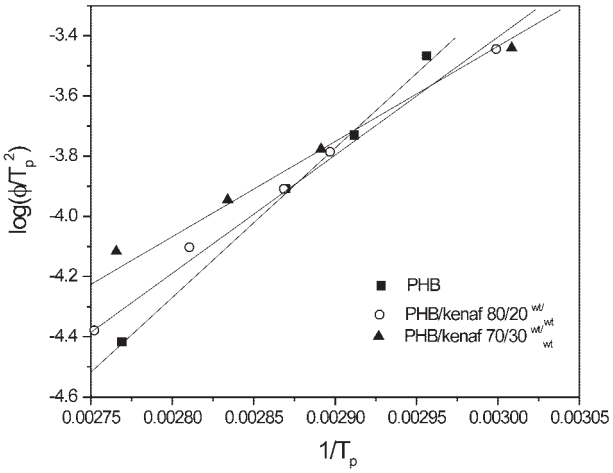

Figure 6 Kissinger plots for the evaluation of the nonisothermal crystallization energies for PHB and its model composites with kenaf fibers.

If we turn off to the kinetic results obtained from the Avrami analysis (Table II), it can be concluded that the crystallization rates of PHB are almost independent of the fiber content; this is the opposite of the conclusions based on the Mo analysis. This is the case because the Avrami approach for nonisothermal crystallization collects data related to low and high relative crystallization, whereas the Mo analysis gives the crystallization functions related to certain x_c values. From this point of view, the different nonisothermal treatments of the data must be considered with care.

Plots of $(\ln \phi/T_p^2)$ versus $1/T$ are shown in Figure 6. The crystallization activation energies were determined from the slope of the obtained straight lines. A higher activation energy of 41.2 kJ/mol was obtained for the pure polymer resin, compared with the activation energies of 32.6 and 26.3 kJ/mol for the 80/20 and 70/30 PHB/kenaf fiber composites, respectively. This could be evidence that in these composite materials the crystallization is relieved because of the nucleation effect of the kenaf fibers.

Reinsch and Kelley[19] reported similar nucleating activity for wood fibers for the crystallization process of the PHBV resin.[19] In contrast to this, Luo and Netravali[18] found that pineapple fibers did not affect the crystallization kinetics of the PHBV matrix.

The nucleating activity of the kenaf fibers can also be confirmed by the transcrystalline morphology of the PHB that develops on the fiber surface (Fig. 7). When PHB is allowed to cool in contact with kenaf fiber, which is a source of nucleating centers, the crystallization develops in a direction perpendicular to the fiber surface. In the literature, a similar ability of different fibers and fillers to induce transcrystallinity in various composites has been reported.[36]

TABLE III
Values of the a and F(T) Parameters Versus X_t Based on the Mo Treatment for PHB and Its Composites with Kenaf Fibers

			PHB/kenaf			
	PHB		80/20 w/w		70/30 w/w	
X_t (%)	$F(T)$	a	F(T)	a	F(T)	a
20	31.4	1.04	30.4	1.39	27.5	1.15
40	40.6	1.07	42.0	1.42	36.3	1.24
60	48.9	1.08	53.1	1.44	44.6	1.28
80	58.8	1.08	68.7	1.49	54.9	1.31

CONCLUSIONS

The nonisothermal crystallization kinetics of PHB in PHB/kenaf fiber composites were investigated with DSC at cooling rates ranging from 5 to 40°/min. The crystallization behavior was analyzed by the Avrami,

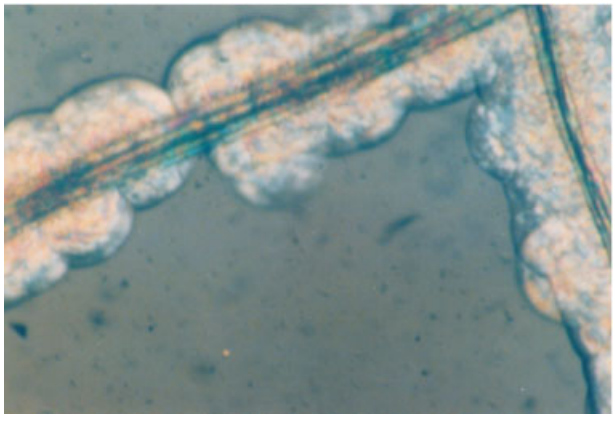

Figure 7 Transcrystallinity in PHB/kenaf fiber composites. [Color figure can be viewed in the online issue, which is available at www.interscience.wiley.com.]

Ozawa, and Mo methods. The Ozawa analysis was inapplicable for a treatment of the experimental results. In contrast, the modified Avrami method gave satisfactory results together with the Mo analysis. The Avrami analysis suggested that secondary crystallization did not occur in these systems. The activation energies of the composites were lower, compared with that of the pure PHB matrix, and this suggested that the fiber lowered the effective energy barrier of crystallization.

References

1. Selke, S. Biodegradation and Packaging, 2nd ed.; Pira International Reviews: Leatherhead, Surrey, 1996.
2. Avella, M.; Bonadies, E.; Martuscelli, E.; Rimedio, R. Polym Test 2001, 20, 517.
3. Albertsson, A. C.; Karlsson, S. Acta Polym 1995, 46, 114.
4. Furukawa, T.; Matsusue, Y.; Yasunaga, T.; Shikinami, Y.; Okuno, M.; Nakamura, T. Biomaterials 2000, 21, 889.
5. Barham, P. J.; Keller, A.; Otun, E. L.; Holmes, P. A. J Mater Sci 1984, 19, 2781.
6. Organ, S. J.; Barham, P. J. Polymer 1993, 34, 2169.
7. Bauer, H.; Owen, A. J. Colloid Polym Sci 1988, 266, 241.
8. Shimamura, E.; Kasuya, K.; Kobayashi, C.; Shiotani, T.; Shima, Y.; Doy, Y. Macromolecules 1994, 27, 878.
9. Verhoogt, H.; Ramsay, B. A.; Favis, B. D. Polymer 1994, 35, 5155.
10. Avella, M.; Martuscelli, E.; Raimo, M. J Mater Sci 2000, 35, 523.
11. Greco, P.; Martuscelli, E. Polymer 1989, 30, 1475.
12. Avella, M.; Focher, B.; Martuscelli, E.; Marzetti, A.; Pascucci, B.; Raimo, M. J Appl Polym Sci 1993, 49, 2091.
13. Gatenholm, P.; Mathiasson, A. J Appl Polym Sci 1994, 51, 1231.
14. Mohanty, A. K.; Khan, M. A.; Sahoo, S.; Hinrichsen, G. J Mater Sci 2000, 35, 2589.
15. Luo, S.; Netravali, A. N. J Mater Sci 1999, 34, 3709.
16. Avella, M.; Martuscelli, E. Polymer 1988, 29, 1731.
17. Avella, M.; Martuscelli, E.; Greco, P. Polymer 1991, 32, 1647.
18. Luo, S.; Netravali, A. N. Polym Compos 1999, 20, 367.
19. Reinsch, V. E.; Kelley, S. S. J Appl Polym Sci 1997, 64, 1785.
20. Reinsch, V. E.; Rebenfeld, L. J Appl Polym Sci 1994, 52, 649.
21. Mehl, N. A.; Rebenfeld, L. J Polym Sci Part B: Polym Phys 1993, 31, 1687.
22. Biddlestone, F.; Harris, A.; Hay, J. N. Polym Int 1996, 39, 221.
23. Avrami, M. J. J Chem Phys 1939, 7, 1103.
24. Avrami, M. J. J Chem Phys 1940, 8, 212.
25. Avrami, M. J. J Chem Phys 1941, 9, 177.
26. Lopez, L. C.; Wilkes, L. G. Polymer 1989, 30, 882.
27. Addonizio, M. L.; Martuscelli, E.; Silvestre, C. Polymer 1987, 28, 183.
28. Patel, R. M.; Bheda, J. H.; Spruiell, J. J Appl Polym Sci 1991, 42, 1671.
29. Jeziorny, A. Polymer 1978, 19, 1142.
30. Ozawa, T. Polymer 1971, 12, 150.
31. Liu, T.; Mo, Z.; Wang, S.; Zhang, H. Polym Eng Sci 1997, 37, 568.
32. Kissinger, H. E. Anal Chem 1957, 11, 1702.
33. Grozdanov, A.; Bogoeva-Gaceva, G. Compos Interfaces 2003, 10, 297.
34. Cimmino, S.; Iodice, P.; Martuscelli, E.; Silvestre, C. Thermochim Acta 1998, 321, 89.
35. An, Y.; Dong, L.; Mo, Z.; Liu. T.; Feng, Z. J Polym Sci Part B: Polym Phys 1998, 36, 1305.
36. Wang, C.; Hwang, L. M. J Polym Sci Part B: Polym Phys 1996, 34, 47.